σ-Acetylide Complexes of Rhodium(I), Rhodium(II), and Rhodium(III). Correlation between Electrochemical ($E^{\circ\prime}$) and Spectroscopic ($\Delta\nu$(C≡C)) Parameters and dπ (Metal) → π* (Acetylide) Transfer

Claudio Bianchini,* Andrea Meli, Maurizio Peruzzini, and Alberto Vacca

Istituto per lo Studio della Stereochimica ed Energetica dei Composti di Coordinazione, CNR, Via J. Nardi 39, 50132 Firenze, Italy

Franco Laschi and Piero Zanello*

Dipartimento di Chimica, Università di Siena, 53100 Siena, Italy

Francesca M. Ottaviani

Dipartimento di Chimica, Università di Firenze, 50100 Firenze, Italy

Received May 25, 1989

Terminal acetylide complexes of rhodium(II) and rhodium(III) with the tripodal polyphosphine ligands $N(CH_2CH_2PPh_2)_3$ (NP_3) and $P(CH_2CH_2PPh_2)_3$ (PP_3) have been synthesized either by controlled-potential coulometry or by chemical oxidation of the Rh(I) neutral σ-acetylide compounds [(L)Rh(C≡CR)] (L = NP_3, R = Ph, CO_2Et; L = PP_3, R = Ph, CO_2Et, CHO). All of the compounds undergo electron-transfer reactions that encompass the Rh(I), Rh(II), and Rh(III) oxidation states of the metal. The characterization has been carried out by IR, NMR, and ESR techniques. The presence of a significant dπ (metal) → π* (acetylide) interaction in the HOMO is diagnosed by comparing and contrasting either the stretching frequencies ν(C≡C) within the members of the $[(L)Rh(C{\equiv}CR)]^{n+}$ family (n = 0–2) or the redox potentials $E^{\circ\prime}$ within the more numerous [(L)RhX] family (X = Cl, H, C≡CR, CN, CO).

Introduction

Over the past decade, intense research activity has been expended on transition-metal σ-acetylide complexes.[1-10] Much of the interest in these organometallics stems from the ease with which the σ-acetylide ligand can be introduced into complex frameworks and successively functionalized.[11-14] Also, σ-acetylide complexes are becoming increasingly important in several applied areas, including organic and organometallic syntheses,[15-21] homogeneous and heterogeneous catalysis,[13,22] and preparation of unidimensional materials.[23]

Considerable progress has been made in understanding the chemistry of σ-acetylide complexes. It is now clear that the great reactivity of these compounds is a direct consequence of their unsaturation coupled with susceptibility to nucleophilic attack at the C_α carbon and electrophilic attack at the C_β carbon.[19e,24] Also, it is now evident that these effects can be finely tuned by purposeful variation of the steric and electronic properties of the C_β substituent as well as the nature of the supporting metal fragment. It is therefore surprising that, surveying the literature on transition-metal σ-acetylides, one finds that a crucial point regarding the nature of the M—C≡CR bond is still a questionable matter. In particular, it has not been established as yet in which cases and to what extent one should expect back-bonding from the metal to the alkynyl species.[1] In fact, even for those cases in which symmetry arguments are consistent with back-donation, theoretical

(1) Reviews: (a) Nast, R. *Coord. Chem. Rev.* **1982**, *47*, 89. (b) Carty, A. J. *Pure Appl. Chem.* **1982**, *54*, 113. (c) Rauthby, P. R.; Rosales, M. J. *Adv. Inorg. Chem. Radiochem.* **1985**, *29*, 169. (d) Sappa, E.; Tiripicchio, A.; Braunstein, P. *Coord. Chem. Rev.* **1985**, *65*, 219.

(2) Appel, M.; Heidrich, J.; Beck, W. *Chem. Ber.* **1987**, *120*, 1087 and references cited therein.

(3) Senn, D. R.; Wong, A.; Patton, A. T.; Marsi, M.; Strouse, C. E.; Gladysz, J. A. *J. Am. Chem. Soc.* **1988**, *110*, 6096 and references cited therein.

(4) Pombeiro, A. J. L. *J. Organomet. Chem.* **1988**, *358*, 273.

(5) Wood, G. L.; Knoebler, C. B.; Hawthorne, M. F. *Inorg. Chem.* **1989**, *28*, 382.

(6) Gamasa, M. P.; Gimeno, J.; Lastra, E.; Solans, X. *J. Organomet. Chem.* **1988**, *346*, 277.

(7) Nickias, P. N.; Selegue, J. P.; Young, B. A. *Organometallics* **1988**, *7*, 2248.

(8) Bullock, R. M. *J. Chem. Soc., Chem. Commun.* **1989**, 165.

(9) Cherkas, A. A.; Randall, R. H.; MacLaughin, S. A.; Mott, G. N.; Taylor, N. J.; Carty, A. J. *Organometallics* **1988**, *7*, 969.

(10) Buang, N. A.; Hughes, D. L.; Kashef, N.; Richards, R. L.; Pombeiro, A. J. L. *J. Organomet. Chem.* **1987**, *323*, C47.

(11) Bruce, M. I. *Pure Appl. Chem.* **1986**, *58*, 553.

(12) Nicholas, K. M.; Nestle, M. O.; Seyferth, D. In *Transition Metal Organometallics in Organic Synthesis*; Alper, H., Ed.; Academic Press: New York, 1978; Vol. II, Chapter I.

(13) Otsuka, S.; Nakamura, A. *Adv. Organomet. Chem.* **1976**, *14*, 245.

(14) Hubel, W. In *Organic Synthesis via Metal Carbonyls*; Wender, I., Pino, P., Eds.; Wiley: New York, 1968; Vol. I.

(15) Hills, A.; Hughes, D. L.; Kashef, N.; Richards, R. L.; Lemos, M. A. N. D. A.; Pombeiro, A. J. L. *J. Organomet. Chem.* **1988**, *350*, C4.

(16) (b) Bruce, M. I.; Liddell, M. J.; Snow, M. R.; Tiekink, E. R. T. *J. Organomet. Chem.* **1988**, *354*, 343. (b) *Ibid.* **1988**, *352*, 199. (c) Selegue, J. P. *J. Am. Chem. Soc.* **1982**, *104*, 119.

(17) (a) Bruce, M. I.; Liddell, M. J.; Snow, M. R.; Tiekink, E. R. T. *Organometallics* **1988**, *7*, 343. (b) Bruce, M. I.; Duffy, D. N.; Liddell, M. J.; Snow, M. R.; Tiekink, E. R. T. *J. Organomet. Chem.* **1987**, *335*, 365.

(18) (a) Bell, M. I.; Chisholm, M. H.; Couch, D. A.; Rankel, A. *Inorg. Chem.* **1977**, *16*, 687.

(19) (a) Bruce, M. I.; Koutsantonis, G. A.; Liddell, M. J.; Nicholson, B. K. *J. Organomet. Chem.* **1987**, *320*, 217. (b) Bruce, M. I.; Humphry, M. G.; Liddell, M. J. *Ibid.* **1987**, *321*, 91. (c) Bruce, M. I.; Koutsantonis, G. A.; Humphry, M. G.; Liddell, M. J. *Ibid.* **1987**, *326*, 247. (d) Abbott, S.; Davies, S. G.; Warner, J. *Ibid.* **1983**, *246*, C65. (e) Bruce, M. I.; Swincer, A. G. *Adv. Organomet. Chem.* **1983**, *22*, 59.

(20) (a) Wong, Y. S.; Paik, H. N.; Chieh, P. C.; Carty, A. J. *J. Chem. Soc., Chem. Commun.* **1975**, *309*. (b) Carty, A. J.; Taylor, N. J.; Paik, H. N.; Smith, W.; Yule, J. G. *Ibid.* **1976**, 41. (c) Mott, G. N.; Carty, A. J. *Inorg. Chem.* **1983**, *22*, 2726. (d) Carty, A. J.; Taylor, N. J.; Sappa, E.; Tiripicchio, A. *Ibid.* **1983**, *22*, 1871.

(21) (a) Birdwhistell, K. R.; Templeton, J. L. *Organometallics* **1985**, *4*, 2062. (b) Weinand, R.; Werner, H. *J. Chem. Soc., Chem. Commun.* **1985**, 1145. (c) Mayr, A.; Schaefer, K. C.; Huang, E. Y. *J. Am. Chem. Soc.* **1984**, *106*, 1517.

(22) (a) Brown, C. K.; Georgiou, D.; Wilkinson, G. *J. Chem. Soc. A* **1971**, 3120. (b) Moulijin, J. A.; Reitsma, H. J.; Boelhouwer, C. *J. Catal.* **1972**, *25*, 434. (c) Berry, D. H.; Eisenberg, R. *Organometallics* **1987**, *6*, 1796 and references cited therein.

(23) Sonogashira, K.; Ohga, K.; Takahashi, S.; Hagihara, N. *J. Organomet. Chem.* **1980**, *188*, 237.

(24) Kostic, N. M.; Fenske, R. *Organometallics* **1982**, *1*, 974.

0276-7333/90/2309-0360$02.50/0

Table I. $^{31}P\{^1H\}$ NMR Data for the Rh(III) σ-Acetylide Complexes[a]

complex	solvent	T, K	isomer[c]	chem shift, ppm			coupling const, Hz					
				P_A	P_M	P_Q	$J_{P_AP_M}$	$J_{P_AP_Q}$	$J_{P_MP_Q}$	J_{P_ARh}	J_{P_MRh}	J_{P_QRh}
8	CD_2Cl_2	298		35.45	28.11		22.0			118.5	91.3	
8a,b	CD_2Cl_2	298		36.20	29.07		22.0			127.9	88.1	
				34.12	24.49		21.9			128.1	87.8	
8c	CD_3COCD_3	298		35.70	23.81		b			136.5	84.9	
		188	α	32.08	21.91		22.5			129.4	89.7	
			β	36.38	25.38		23.3			127.7	90.1	
9a,c	CD_2Cl_2	298	α	36.13	32.99		22.1			115.2	92.1	
			β	34.77	33.27		22.2			115.4	92.2	
9b,d	CD_3COCD_3	298		37.87	27.42		b			130.9	84.2	
		218	α	36.14	27.23		21.7			127.0	88.5	
			β	39.32	30.05		21.9			125.0	88.4	
13, 13a	CD_2Cl_2	298		140.85	39.58		0			109.9	86.2	
		213		140.18	37.85	39.12	0	1.8	21.5	106.9	84.8	89.2
14, 14a	CD_2Cl_2	298		132.60	33.12		0			106.1	86.3	
		203		131.98	32.08	33.29	0	2.4	21.8	107.2	84.8	88.6
15	CD_3COCD_3	298	α	143.77	42.60	38.30	0	0	21.1	109.3	82.6	89.0
			β	143.09	41.91	40.74	0	0	21.1	107.7	84.3	88.8
16	CD_3COCD_3	298	α	134.07	30.39	33.20	0	3.6	22.1	105.9	83.0	88.0
			β	134.65	32.07	29.40	0	0	22.2	107.2	83.9	87.9

[a] Chemical shifts (δ) are relative to 85% H_3PO_4, with positive values being downfield from the standard. The compounds 8, 8a, 8c, 9a, 9b, 13, 14, 15, and 16 exhibit the high-field PF_6^- septuplet in the expected position. [b] Not resolved. [c] The symbols α and β stand for two conformational isomers (see text).

calculations predict that the metal to ligand electron transfer may be scarce or even absent because of the high energy of the π* level of the acetylide.[24]

Intuitively, the dπ (metal) → π* (ligand) transfer should be favored for transition metals located at the right side of the periodic table, preferentially in a low oxidation state, as well as for C_β substituents with electron-withdrawing character. The σ-acetylide complexes of rhodium(I) $[(NP_3)Rh(C{\equiv}CR)]$ (R = Ph (1), CO_2Et (2)) and $[(PP_3)Rh(C{\equiv}CR)]$ (R = Ph (3), CO_2Et (4), CHO (5)), which inspired this work,[25] appeared to be appropriately designed to satisfy the two requirements, and actually, in this paper and in a future one, we demonstrate experimentally that back-donation makes an important contribution to both their stabilization and chemistry (NP_3 = $N(CH_2CH_2PPh_2)_3$; PP_3 = $P(CH_2CH_2PPh_2)_3$).

Experimental Section

General Data. All the reactions and manipulations were routinely performed under a nitrogen or argon atmosphere with standard Schlenk tube techniques. The σ-acetylide complexes $[(NP_3)Rh(C{\equiv}CR)]$ (R = Ph (1), CO_2Et (2)) and $[(PP_3)Rh(C{\equiv}CR)]$ (R = Ph (3), CO_2Et (4), CHO (5)) were prepared as described in ref 25. Ferrocenium hexafluorophosphate was prepared according to the literature method.[26] All the other chemicals were reagent grade and were used as received by commercial suppliers. Tetrahydrofuran, THF, was purified by distillation over $LiAlH_4$ under nitrogen just prior to use. Benzene, *n*-hexane, and *n*-heptane were dried over sodium, dichloromethane and chloroform were dried over P_2O_5, and acetone was dried over K_2CO_3. They were, similarly, purified by distillation under a nitrogen atmosphere. Infrared spectra were recorded on a Perkin-Elmer 1600 Series FTIR instrument using samples mulled in Nujol between KBr plates. Proton NMR spectra were recorded at 299.945 MHz on a Varian VXR 300 spectrometer. The chemical shifts are reported relative to tetramethylsilane as external reference or calibrated against the solvent as the reference signal. $^{31}P\{^1H\}$ NMR spectra were recorded on Varian CFT 20 and Varian VXR 300 spectrometers operating at 32.19 and 121.42 MHz, respectively. Chemical shifts are relative to external 85% H_3PO_4, with downfield values reported as positive. The simulation of the $^{31}P\{^1H\}$ NMR spectra was carried out by using an updated version of the LAOCN4 program.[27] The initial choices of shifts and coupling constants were refined by successive iterations, the assignment of the experimental lines being performed automatically. The final parameters gave a fit to the observed line positions better than 0.5 Hz. Conductivities were measured with a WTW Model LBR/B conductivity bridge. The conductivity data were obtained at sample concentrations of ca. 10^{-3} M in nitromethane solutions at room temperature. Magnetic susceptibilities of solid samples were measured on a Faraday balance. The materials and the apparatus used for the electrochemical experiments have been described elsewhere.[28] The potential values are relative to an aqueous calomel electrode (SCE) and refer to a controlled temperature of 20 ± 0.1 °C. Reaction entropies obtained from the temperature dependence of the formal potential have been measured by using a nonisothermal cell arrangement.[29] Under the present experimental conditions, the ferrocenium/ferrocene couple was located at +0.49 V in CH_2Cl_2 solution and at +0.56 V in THF solution. X-Band ESR spectra were recorded with a Bruker ER 200-SRCB spectrometer operating at ω° = 9.78 GHz. The control of the external magnetic field was obtained with a microwave bridge ER 041 MR (Bruker) wave meter. The temperature was varied and controlled with a Bruker ER 4111 VT device with an accuracy of ±1 °C. In order to estimate accurate g_{iso} and g_{aniso} values over the temperature range of interest, the diphenylpicrylhydrazyl free radical (DPPH) was used as a field marker (g_{iso}(DPPH) = 2.0036). In order to assure quantitative reproducibility, the samples were placed in calibrated quartz capillary tubes permanently positioned in the resonance cavity. The ESR spectra were simulated by the computer program SL, which takes into account the line-width dependence on the m_i values for each group of equivalent nuclei.[30]

Synthesis of the Complexes. The solid compounds were collected on sintered-glass frits and washed, unless otherwise stated, with ethanol and *n*-pentane before being dried under a stream of nitrogen.

Selected NMR and IR spectral data for all the new complexes are collected in Table I ($^{31}P\{^1H\}$ NMR spectra) and Table II (IR spectra).

Preparation of $[(NP_3)Rh(C{\equiv}CR)]ClO_4$ (R = Ph (6), CO_2Et (7)). Complex 1 (0.45 g, 0.52 mmol) dissolved in a 0.2 M THF solution of $[NBu_4]ClO_4$ as supporting electrolyte (20 mL) was exhaustively electrolyzed at −0.2 V. At the end of the electrolysis, the solution was greenish and yellow-green microcrystals of 6

(25) Bianchini, C.; Masi, D.; Meli, A.; Peruzzini, M.; Ramirez, J. A.; Vacca, A.; Zanobini, F. *Organometallics* **1989**, *8*, 2179.
(26) Smart, J. C.; Pinsky, B. L. *J. Am. Chem. Soc.* **1980**, *102*, 1009.
(27) Castellano, S.; Bothner-By, A. A. *J. Chem. Phys.* **1964**, *41*, 3863.
(28) Bianchini, C.; Mealli, C.; Meli, A.; Sabat, M.; Zanello, P. *J. Am. Chem. Soc.* **1987**, *109*, 185.
(29) Hupp, J. T.; Weaver, M. J. *Inorg. Chem.* **1984**, *23*, 3639.
(30) (a) Ottaviani, M. F. *J. Phys. Chem.* **1987**, *91*, 779. (b) Romanelli, M. *Ibid.* **1984**, *88*, 1663.

Table II. ν(C≡C) Stretch for the Rh(I), Rh(II), and Rh(III) σ-Acetylide (C≡CR) Complexes

	ν(C≡C), cm^{-1}			$\Delta\nu$(C≡C),[a] cm^{-1}		
	R = Ph	R = COOEt	R = CHO	R	$Rh_{II/I}$	$Rh_{III/II}$
			NP_3 Complexes			
Rh(I)[b]	2080	2050		Ph	35	10
Rh(II)	2115	2080		COOEt	30	15
Rh(III)	2125	2095				
			PP_3 Complexes			
Rh(I)[b]	2070	2050	2065	Ph	30	15
Rh(II)	2100	2085	2095	COOEt	35	10
Rh(III)	2115	2095		CHO	30	

[a] $\Delta\nu$(C≡C) = $\nu(C{\equiv}C)_{ox} - \nu(C{\equiv}C)_{red}$. [b] Reference 25.

separated after addition of an ethanol/*n*-heptane mixture (30 mL, 1:1 v/v); yield 95%. Λ_M = 75 Ω^{-1} cm^2 mol^{-1}. IR: ν(C≡C) 2115 cm^{-1}; phenyl reinforced vibration 1590 cm^{-1}. μ_{eff} = 1.90 μ_B. Anal. Calcd for $C_{50}H_{47}ClNO_4P_3Rh$: C, 62.75; H, 4.95; N, 1.46; Rh, 10.75. Found: C, 62.42; H, 5.03; N, 1.36; Rh, 10.69.

The acetylide **7** was obtained in 90% yield by substituting **2** for **1** in the above procedure. Λ_M = 82 Ω^{-1} cm^2 mol^{-1}. IR: ν(C≡C) 2080 cm^{-1}; ν(CO) 1680 cm^{-1}; ν(C—O—C) 1190 cm^{-1}. μ_{eff} = 1.85 μ_B. Anal. Calcd for $C_{47}H_{47}ClNO_6P_3Rh$: C, 59.23; H, 4.97; N, 1.47; Rh, 10.80. Found: C, 59.00; H, 4.99; N, 1.32; Rh, 10.66.

Preparation of [(NP$_3$)Rh(C≡CR)]BF$_4$ (R = Ph (6a), CO$_2$Et (7a)). To a stirred suspension of **1** (0.20 g, 0.24 mmol) in THF (25 mL) was added 1 equiv of solid $AgBF_4$ (0.05 g, 0.26 mmol) with vigorous stirring. Addition of ethanol (30 mL) and concentration under a stream of nitrogen gave **6a** as clear yellow-green microcrystals, yield 75%. Λ_M = 78 Ω^{-1} cm^2 mol^{-1}. IR: ν(C≡C) 2115 cm^{-1}; phenyl reinforced vibration 1590 cm^{-1}. μ_{eff} = 1.90 μ_B. Anal. Calcd for $C_{50}H_{47}BF_4NP_3Rh$: C, 63.59; H, 5.02; N, 1.48; Rh, 10.90. Found: C, 63.38; H, 4.94; N, 1.33; Rh, 10.80.

The carboethoxy derivative **7a** was prepared in 80% yield by substituting **2** for **1**. Λ_M = 80 Ω^{-1} cm^2 mol^{-1}. IR: ν(C≡C) 2080 cm^{-1}; ν(CO) 1680 cm^{-1}; ν(C—O—C) 1195 cm^{-1}. μ_{eff} = 1.90 μ_B. Anal. Calcd for $C_{47}H_{47}BF_4NO_2P_3Rh$: C, 60.03; H, 5.04; N, 1.49; Rh, 10.94. Found: C, 59.85; H, 4.97; N, 1.32; Rh, 10.67.

Preparation of [(NP$_3$)Rh(C≡CR)]PF$_6$ (R = Ph (6b), CO$_2$Et (7b)). To a stirred solution of **1** (0.20 g, 0.24 mmol) in CH_2Cl_2 (25 mL) was added 1 equiv of solid $[(C_5H_5)_2Fe]PF_6$ (0.08 g, 0.24 mmol) with vigorous stirring. Addition of ethanol (30 mL) and concentration under a stream of nitrogen gave pale yellow crystals of **6b**, yield 80%. Λ_M = 84 Ω^{-1} cm^2 mol^{-1}. IR: ν(C≡C) 2115 cm^{-1}; phenyl reinforced vibration 1595 cm^{-1}. μ_{eff} = 1.85 μ_B. Anal. Calcd for $C_{50}H_{47}F_6NP_4Rh$: C, 59.90; H, 4.72; N, 1.40; Rh, 10.26. Found: C, 59.73; H, 4.68; N, 1.37; Rh, 10.02.

The alkynyl complex **7b** was prepared by the same procedure used for **7a**, with **2** instead of **1**. Λ_M = 79 Ω^{-1} cm^2 mol^{-1}. IR: ν(C≡C) 2080 cm^{-1}; ν(CO) 1680 cm^{-1}; ν(C—O—C) 1190 cm^{-1}. μ_{eff} = 1.85 μ_B. Anal. Calcd for $C_{47}H_{47}F_6NO_2P_4Rh$: C, 56.59; H, 4.75; N, 1.40; Rh, 10.32. Found: C, 56.46; H, 4.77; N, 1.40; Rh, 10.22.

Preparation of [(NP$_3$)Rh(C≡CPh)](PF$_6$)$_2$ (8). Method A. Solid $[(C_5H_5)_2Fe]PF_6$ (0.31 g, 0.94 mmol) was added with vigorous stirring to a CH_2Cl_2 solution (30 mL) solution of **1** (0.40 g, 0.47 mmol). The stirring was continued for 30 min while the color gradually turned to orange. Addition of *n*-hexane gave cream-colored microcrystals of **8**. The product was washed with *n*-pentane before being dried under a stream of nitrogen; yield 90%.

Method B. One equivalent of $[(C_5H_5)_2Fe]PF_6$ (0.07 g, 0.21 mmol) was added with vigorous stirring to a CH_2Cl_2 solution (20 mL) of **6b** (0.20 g, 0.20 mmol). Addition of *n*-hexane (40 mL) precipitated pale cream-colored microcrystals of **8**, yield 90%. Λ_M = 152 Ω^{-1} cm^2 mol^{-1}. IR: ν(C≡C) 2125 cm^{-1}; phenyl reinforced vibration 1600 cm^{-1}. Anal. Calcd for $C_{48}H_{47}F_{12}NP_5Rh$: C, 50.24; H, 4.13; N, 1.22; Rh, 8.97. Found: C, 50.07; H, 4.11; N, 1.07; Rh, 8.74.

Preparation of [(NP$_3$)Rh(C≡CPh)(C$_2$H$_5$OH)](PF$_6$)$_2$ (8a). Compound **8a** was synthesized by the above procedures with use of ethanol (30 mL) instead of *n*-hexane. The yields of **8a** were 80% (method A) and 70% (method B). Λ_M = 148 Ω^{-1} cm^2 mol^{-1}. IR: $\nu(OH)_{EtOH}$ 3460 cm^{-1}; ν(C≡C) 2125 cm^{-1}; phenyl reinforced vibration 1600 cm^{-1}. Anal. Calcd for $C_{50}H_{53}F_{12}NOP_5Rh$: C, 50.32; H, 4.48; N, 1.17; Rh, 8.62. Found: C, 50.16; H, 4.39; N, 1.09; Rh, 8.60.

Preparation of [(NP$_3$)Rh(C≡CPh)(C$_2$H$_5$OH)](BF$_4$)$_2$ (8b). Method A. Solid $AgBF_4$ (0.18 g, 0.94 mmol) was added with vigorous stirring to a THF (30 mL) suspension of **1** (0.40 g, 0.47 mmol). The reaction mixture was stirred for 30 min and carefully filtered to eliminate silver. Upon addition of ethanol (30 mL) to the resulting clear yellow solution, yellow microcrystals of **8b** separated; yield 80%.

Method B. Solid $AgBF_4$ (0.04 g, 0.21 mmol) was added with vigorous stirring to a THF solution (20 mL) of **6a** (0.20 g, 0.21 mmol). Workup as above gave **8b** in ca. 70% yield. Λ_M = 149 Ω^{-1} cm^2 mol^{-1}. IR: $\nu(OH)_{EtOH}$ 3450 cm^{-1}; ν(C≡C) 2125 cm^{-1}; phenyl reinforced vibration 1600 cm^{-1}. Anal. Calcd for $C_{50}H_{53}B_2F_8NOP_3Rh$: C, 55.75; H, 4.96; N, 1.30; Rh, 9.55. Found: C, 55.61; H, 4.99; N, 1.27; Rh, 9.44.

Preparation of [(NP$_3$)Rh(C≡CPh)(CH$_3$COCH$_3$)](PF$_6$)$_2$ (8c). The acetone complex **8c** was obtained by recrystallization of **8** or **8a** from acetone/ethanol mixtures; yield 95%. Λ_M = 152 Ω^{-1} cm^2 mol^{-1}. IR: ν(C≡C) 2125 cm^{-1}; $\nu(CO)_{acetone}$ 1720 cm^{-1}. Anal. Calcd for $C_{51}H_{53}F_{12}NOP_5Rh$: C, 50.81; H, 4.43; N, 1.16; Rh, 8.54. Found: C, 50.49; H, 4.58; N, 1.07; Rh, 8.29.

Preparation of [(NP$_3$)Rh(C≡CCO$_2$Et)(C$_5$H$_5$OH)]Y$_2$ (Y = PF$_6$ (9a), BF$_4$ (9c)). The ethanol adducts **9a** and **9c**, containing the (ethoxycarbonyl)acetylide ligand, were prepared as described above for the phenylacetylide analogues **8a,b** with use of **2** instead of **1** or **7a,b** instead of **6a,b**.

9a: yield 90% (method A), 80% (method B). Λ_M = 151 Ω^{-1} cm^2 mol^{-1}. IR: $\nu(OH)_{EtOH}$ 3450 cm^{-1}; ν(C≡C) 2095 cm^{-1}; ν(CO) 1685 cm^{-1}; ν(C—O—C) 1230 cm^{-1}. ^{1}H NMR (299.945 MHz, CD_2Cl_2, 298 K, TMS reference): 4.48 ppm (q, 2 H, J_{HH} = 7.1 Hz); 1.22 ppm (t, 3 H). Anal. Calcd for $C_{49}H_{53}F_{12}NO_3P_5Rh$: C, 49.47; H, 4.49; N, 1.18; Rh, 8.65. Found: C, 49.28; H, 4.57; N, 1.08; Rh, 8.49.

9c: yield 85% (method A), 80% (method B). Λ_M = 144 Ω^{-1} cm^2 mol^{-1}. IR: $\nu(OH)_{EtOH}$ 3450 cm^{-1}; ν(C≡C) 2095 cm^{-1}; ν(CO) 1680 cm^{-1}; ν(C—O—C) 1230 cm^{-1}. ^{1}H NMR (299.945 MHz, CD_2Cl_2, 298 K, TMS reference): 4.48 ppm (q, 2 H, J_{HH} = 7.1 Hz); 1.22 ppm (t, 3 H). Anal. Calcd for $C_{49}H_{53}B_2F_8NO_3P_5Rh$: C, 54.84; H, 4.98; N, 1.31; Rh, 9.59. Found: C, 54.60; H, 4.90; N, 1.22; Rh, 9.42.

Preparation of [(NP$_3$)Rh(C≡CCO$_2$Et)(CH$_3$COCH$_3$)]Y$_2$ (Y = PF$_6$ (9b), BF$_4$ (9d)). The two acetone adducts **9b** and **9d** were obtained by recrystallization of the ethanol adducts **9a** and **9c**, respectively, from acetone/ethanol mixtures.

9b: yield 95%. Λ_M = 150 Ω^{-1} cm^2 mol^{-1}. IR: ν(C≡C) 2095 cm^{-1}; $\nu(CO)_{acetone}$ 1720 cm^{-1}; $\nu(CO)_{COOEt}$ 1680 cm^{-1}; ν(C—O—C) 1230 cm^{-1}. ^{1}H NMR (299.945 MHz, CD_2Cl_2, 298 K, TMS reference): 4.19 ppm (q, 2 H, J_{HH} = 7.0 Hz); 1.20 ppm (t, 3 H). Anal. Calcd for $C_{50}H_{53}F_{12}NO_3P_5Rh$: C, 49.98; H, 4.45; N, 1.17; Rh, 8.56. Found: C, 49.77; H, 4.52; N, 1.06; Rh, 8.40.

9d: yield 95%. Λ_M = 148 Ω^{-1} cm^2 mol^{-1}. IR: ν(C≡C) 2095 cm^{-1}; $\nu(CO)_{acetone}$ 1720 cm^{-1}; $\nu(CO)_{COOEt}$ 1680 cm^{-1}; ν(C—O—C) 1235 cm^{-1}. ^{1}H NMR (299.945 MHz, CD_2Cl_2, 298 K, TMS reference): 4.19 ppm (q, 2 H, J_{HH} = 7.0 Hz); 1.20 ppm (t, 3 H). Anal. Calcd for $C_{50}H_{53}B_2F_8NO_3P_3Rh$: C, 55.34; H, 4.92; N, 1.29; Rh, 9.48. Found: C, 55.26; H, 4.98; N, 1.19; Rh, 9.39.

Preparation of [(PP$_3$)Rh(C≡CR)]ClO$_4$ (R = Ph (10), CO$_2$Et (11), CHO (12)). The PP_3 complexes **10–12** were prepared by controlled-potential coulometry in THF at −0.1 V, with use of the acetylides **3–5** as starting reagents.

10: yield 95%. Λ_M = 81 Ω^{-1} cm^2 mol^{-1}. IR: ν(C≡C) 2100 cm^{-1}; phenyl reinforced vibration 1590 cm^{-1}. μ_{eff} = 1.90 μ_B. Anal. Calcd for $C_{50}H_{47}ClO_4P_4Rh$: C, 61.66; H, 4.86; Rh, 10.57. Found: C, 61.44; H, 4.94; Rh, 10.41.

11: yield 95%. Λ_M = 82 Ω^{-1} cm^2 mol^{-1}. IR: ν(C≡C) 2085 cm^{-1}; ν(CO) 1670 cm^{-1}; ν(C—O—C) 1190 cm^{-1}. μ_{eff} = 1.90 μ_B. Anal. Calcd for $C_{47}H_{47}ClO_6P_4Rh$: C, 58.20; H, 4.88; Rh, 10.61. Found: C, 58.02; H, 5.07; Rh, 10.45.

12: yield 85%. Λ_M = 77 Ω^{-1} cm^2 mol^{-1}. IR: ν(C≡C) 2095 cm^{-1}; ν(CO) 1600 cm^{-1}. μ_{eff} = 1.85 μ_B. Anal. Calcd for $C_{45}H_{43}ClO_5P_4Rh$: C, 58.36; H, 4.68; Rh, 11.11. Found: C, 58.17; H, 4.67; Rh, 10.91.

Preparation of [(PP$_3$)Rh(C≡CR)]BF$_4$ (R = Ph (10a), CO$_2$Et (11a), CHO (12a)). The tetrafluoroborate salts **10a–12a** were synthesized as described above for the NP_3 analogues **6a** and **7a** by substituting **3–5** for **1** and **2**.

Scheme I

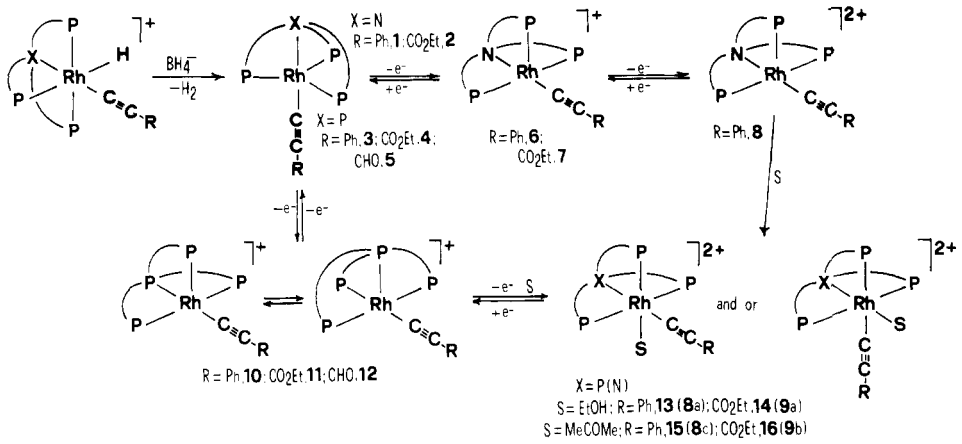

10a: yield 80%. Λ_M = 84 Ω^{-1} cm^2 mol^{-1}. IR: ν(C≡C) 2100 cm^{-1}; phenyl reinforced vibration 1595 cm^{-1}. μ_{eff} = 1.90 μ_B. Anal. Calcd for $C_{50}H_{47}BF_4P_4Rh$: C, 62.47; H, 4.93; Rh, 10.70. Found: C, 62.30; H, 4.98; Rh, 10.66.

11a: yield 85%. Λ_M = 76 Ω^{-1} cm^2 mol^{-1}. IR: ν(C≡C) 2085 cm^{-1}; ν(CO) 1680 cm^{-1}; ν(C—O—C) 1200 cm^{-1}. μ_{eff} = 1.90 μ_B. Anal. Calcd for $C_{47}H_{47}BF_4O_2P_4Rh$: C, 58.98; H, 4.95; Rh, 10.75. Found: C, 58.56; H, 4.82; Rh, 10.42.

12a: yield 70%. Λ_M = 80 Ω^{-1} cm^2 mol^{-1}. IR: ν(C≡C) 2095 cm^{-1}; ν(CO) 1595 cm^{-1}. μ_{eff} = 1.85 μ_B. Anal. Calcd for $C_{45}H_{43}BF_4OP_4Rh$: C, 59.17; H, 4.75; Rh, 11.26. Found: C, 58.99; H, 4.88; Rh, 11.09.

Preparation of [(PP$_3$)Rh(C≡CR)]PF$_6$ (R = Ph (10b), CO$_2$Et (11b), CHO (12b)). The hexafluorophosphate derivatives **10b–12b** were prepared as described above for **6b** and **7b** by employing **3–5** instead of **1** and **2**.

10b: yield 90%. Λ_M = 80 Ω^{-1} cm^2 mol^{-1}. IR: ν(C≡C) 2100 cm^{-1}; phenyl reinforced vibration 1600 cm^{-1}. μ_{eff} = 1.85 μ_B. Anal. Calcd for $C_{50}H_{47}F_6P_5Rh$: C, 58.91; H, 4.65; Rh, 10.09. Found: C, 58,69; H, 4.55; Rh, 10.02.

11b: yield 90%. Λ_M = 80 Ω^{-1} cm^2 mol^{-1}. IR: ν(C≡C) 2085 cm^{-1}; ν(CO) 1670 cm^{-1}; ν(C—O—C) 1190 cm^{-1}. μ_{eff} = 1.90 μ_B. Anal. Calcd for $C_{47}H_{47}F_6O_2P_5Rh$: C, 55.60; H, 4.67; Rh, 10.13. Found: C, 55.43; H, 4.70; Rh, 9.92.

12b: yield 80%. Λ_M = 82 Ω^{-1} cm^2 mol^{-1}. IR: ν(C≡C) 2095 cm^{-1}; ν(CO) 1600 cm^{-1}. μ_{eff} = 1.85 μ_B. Anal. Calcd for $C_{45}H_{43}F_6OP_5Rh$: C, 55.63; H, 4.46; Rh, 10.59. Found: C, 55.44; H, 4.37; Rh, 10.37.

Preparation of [(PP$_3$)Rh(C≡CR)(C$_2$H$_5$OH)]Y$_2$ (R = Ph, Y = PF$_6$ (13), BF$_4$ (13a); R = CO$_2$Et, Y = PF$_6$ (14), BF$_4$ (14a)). The ethanol adducts **13**, **13a**, **14**, and **14a** were obtained in a fashion similar to that described above for the NP$_3$ analogues **8a,b** and **9a,c**.

13: yield 85% (method A), 80% (method B). Λ_M = 149 Ω^{-1} cm^2 mol^{-1}. IR: ν(OH)$_{EtOH}$ 3470 cm^{-1}; ν(C≡C) 2115 cm^{-1}; phenyl reinforced vibration 1590 cm^{-1}. Anal. Calcd for $C_{52}H_{53}F_{12}OP_6Rh$: C, 51.60; H, 4.41; Rh, 8.50. Found: C, 51.45; H, 4.47; Rh, 8.36.

13a: yield 80% (method A), 80% (method B). Λ_M = 149 Ω^{-1} cm^2 mol^{-1}. IR: ν(OH)$_{EtOH}$ 3470 cm^{-1}; ν(C≡C) 2115 cm^{-1}; phenyl reinforced vibration 1595 cm^{-1}. Anal. Calcd for $C_{52}H_{53}B_2F_8OP_4Rh$: C, 57.08; H, 4.88; Rh, 9.40. Found: C, 56.86; H, 4.72; Rh, 9.21.

14: yield 90% (method A), 80% (method B). Λ_M = 149 Ω^{-1} cm^2 mol^{-1}. IR: ν(OH)$_{EtOH}$ 3460 cm^{-1}; ν(C≡C) 2095 cm^{-1}; ν(CO) 1675 cm^{-1}; ν(C—O—C) 1225 cm^{-1}. ^{1}H NMR (299.945 MHz, CD_2Cl_2, 298 K, TMS reference): 3.80 ppm (q, 2 H, J_{HH} = 7.1 Hz); 1.05 ppm (t, 3 H). Anal. Calcd for $C_{49}H_{53}F_{12}O_3P_6Rh$: C, 48.78; H, 4.43; Rh, 8.53. Found: C, 48.49; H, 4.44; Rh, 8.33.

14a: yield 80% (method A) 75% (method B). Λ_M = 142 Ω^{-1} cm^2 mol^{-1}. IR: ν(OH)$_{EtOH}$ 3470 cm^{-1}; ν(C≡C) 2095 cm^{-1}; ν(CO) 1675 cm^{-1}; ν(C—O—C) 1220 cm^{-1}. ^{1}H NMR (299.945 MHz, CD_2Cl_2, 298 K, TMS reference): 3.80 ppm (q, 2 H, J_{HH} = 7.1 Hz); 1.05 ppm (t, 3 H). Anal. Calcd for $C_{49}H_{53}B_2F_8O_3P_4Rh$: C, 53.99; H, 4.90; Rh, 9.44. Found: C, 53.74; H, 5.04; Rh, 9.27.

Preparation of [(PP$_3$)Rh(C≡CR)(CH$_3$COCH$_3$)](PF$_6$)$_2$ (R = Ph (15), CO$_2$Et (16)). The acetone adducts **15** and **16** were obtained by crystallization of the ethanol adducts **13** and **14** respectively, from acetone/ethanol mixtures.

15: yield 95%. Λ_M = 151 Ω^{-1} cm^2 mol^{-1}. IR: ν(C≡C) 2115 cm^{-1}; ν(CO)$_{acetone}$ 1715 cm^{-1}; phenyl reinforced vibration 1600 cm^{-1}. Anal. Calcd for $C_{53}H_{53}F_{12}Op_6Rh$: C, 52.07; H, 4.37; Rh, 8.42. Found: C, 51.89; H, 4.30; Rh, 8.31.

16: yield 95%. Λ_M = 148 Ω^{-1} cm^2 mol^{-1}. IR: ν(C≡C) 2095 cm^{-1}; ν(CO)$_{acetone}$ 1720 cm^{-1}; ν(CO)$_{COOEt}$ 1680 cm^{-1}; ν(C—O—C) 1215 cm^{-1}. ^{1}H NMR (299.945 MHz, CD_2Cl_2, 298 K, TMS reference): 4.02 ppm (q, 2 H, J_{HH} = 7.1 Hz); 1.12 ppm (t, 3 H). Anal. Calcd for $C_{50}H_{53}F_{12}O_3P_6Rh$: C, 49.29; H, 4.38; Rh, 8.45. Found: C, 49.06; H, 4.24; Rh, 8.26.

Reaction of [(L)Rh(C≡CR)]Y$_2$ with LiHBEt$_3$ (L = NP$_3$, PP$_3$; R = Ph, CO$_2$Et; Y = BF$_4$, PF$_6$). (A) 1:1 Reaction. The stoichiometric amount of LiHBEt$_3$ (1.0 M THF solution) was syringed into a stirred THF solution of the appropriate Rh(III) acetylide. Immediately, the solution became yellow (NP$_3$ derivatives) or deep green (PP$_3$ derivatives). Upon addition of ethanol the Rh(II) alkynyls **6a–7b** and **10a–12b** were obtained in ca. 70% yields.

(B) 1:2 Reaction. When the Rh(III) acetylides were reacted with at least a double proportion of LiHBEt$_3$ in THF, yellow crystals of the neutral Rh(I) acetylides **1–4** were obtained upon addition of a volume of ethanol. The yields can be increased to ca. 90% by using a hot ethanolic solution of NaBH$_4$ as reducing reagent.

Results and Discussion

The preparations and the principal reactions of the complexes described in this paper were reported in Scheme I.

Redox Properties of the σ-Acetylide Complexes 1–5. The σ-acetylide complexes of rhodium(I) **1–5** can be prepared as yellow-orange crystals by reaction of the corresponding cis hydride acetylide derivatives in THF with excess NaBH$_4$.[25] All of the compounds have been assigned trigonal-bipyramidal (TBP) structures in which the acetylide ligand is located trans to the bridgehead nitrogen (NP$_3$ complexes) or phorphorus (PP$_3$) atoms of the tripodal ligands. Compounds **1–5** are air-sensitive and must be stored under an inert atmosphere to prevent oxidation.

NP$_3$ Complexes. The cyclic voltammetric response exhibited by **1** in CH_2Cl_2 is reported in Figure 1.

Two subsequent anodic processes (peaks A and B) are displayed, each of which shows a directly associated reduction process (peaks C and D) in the reverse scan. Controlled-potential coulometry at a platinum macroelectrode in correspondence to the first oxidation process (working electrode potential −0.3 V) indicated the consumption of one electron/molecule. Analysis[31] of the cyclic

(31) Brown, E. R.; Large, R. F. In *Physical Methods of Chemistry*; Weiss, A., Berger, A., Rossiter, B. W., Eds.; Wiley: New York, 1971; Part 11A.

Table III. Redox Potentials for the Redox Changes Exhibited by the σ-Acetylide (C≡CR) Complexes of NP_3 and PP_3 in Nonaqueous Solutions[a]

R	$CHCl_2$				THF			
	$E^{\circ\prime}_{+/0}$	ΔE_p[b]	$E^{\circ\prime}_{2+/+}$	ΔE_p[b]	$E^{\circ\prime}_{+/0}$	ΔE_p[b]	$E^{\circ\prime}_{2+/+}$	ΔE_p[b]
				NP_3 Complexes				
C_6H_5	−0.45	150	+0.03	150	−0.43	210	+0.02	210
COOEt	−0.26	170	+0.15	190	−0.26	260	+0.17[c]	
				PP_3 Complexes				
C_6H_5	−0.29	180	+0.38[c]		−0.27	230	+0.31[c]	
CHO	−0.17	170	+0.38[d]	135	−0.16	180	+0.38[c]	
COOEt	−0.21	110	+0.33[d]	170	−0.19	240	+0.28[d]	280

[a] $E^{\circ\prime}$ in volts, ΔE_p in millivolts. [b] Measured at 0.2 V s^{-1}. [c] Peak potential at 0.22 V s^{-1} for irreversible processes. [d] Measured at scan rates for which $i_{pc}/i_{pa} \cong 1$ (see text).

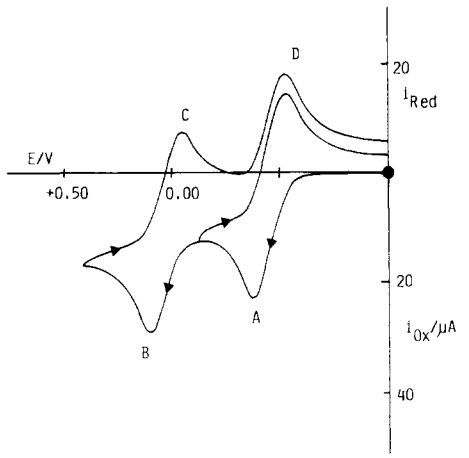

Figure 1. Cyclic voltammogram recorded at a platinum electrode on a deaerated CH_2Cl_2 solution containing 1 (1.70×10^{-3} mol dm^{-3}) and $[NBu_4]ClO_4$ (0.1 mol dm^{-3}) (scan rate 0.2 V s^{-1}).

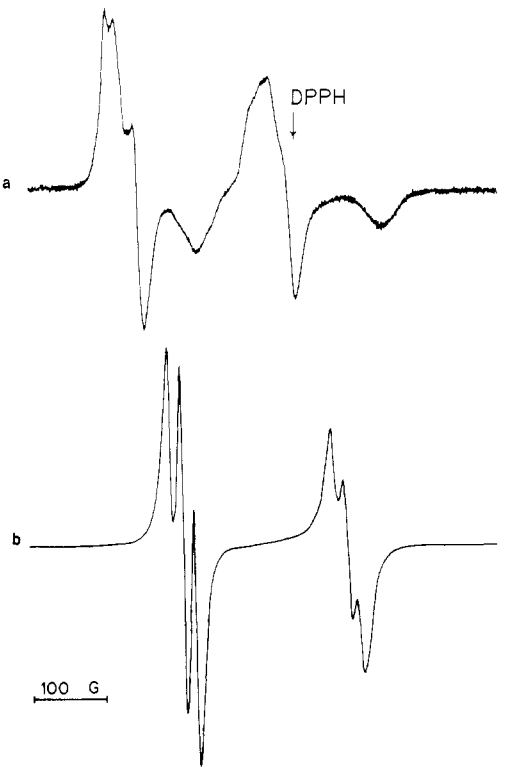

Figure 2. X-Band ESR spectra of electrogenerated $[(NP_3)Rh(C{\equiv}CPh)]^+$ in CH_2Cl_2 at 300 K (b) and 100 K (a).

voltammetric response A/D with scan rates increasing from 0.02 to 10 V s^{-1} (at higher scan rates the voltammograms become ill-defined) reveals the following features: the current ratio i_{pD}/i_{pA} is constantly equal to unity; $i_{pA}v^{-1/2}$ decreases ca. 10%; the difference $E_{pD} - E_{pA}$ increases gradually from 90 to 370 mV (this may be partially due to uncompensated solution resistances). All of these data are diagnostic for a simple quasireversible one-electron-oxidation process. As far as the second peak system B/C is concerned, both the nearness to the first anodic process and the quasireversibility make it difficult to graphically estimate the eventual presence of chemical complications following the charge transfer. However, at the scan rate of 0.02 V s^{-1}, the i_{pC}/i_{pB}, ratio 0.93 indicates that, if present, these coupled homogeneous reactions are rather slow (see below). The same voltammetric picture is observed in THF solution.

Qualitatively similar results are obtained by studying solutions of the carboethoxy acetylide **2**. In conclusion, the electrochemical behavior points out that the main redox changes exhibited by the $[(NP_3)Rh(C{\equiv}CR)]$ systems involve the sequence

$$[(NP_3)Rh(C{\equiv}CR)] \underset{+e^-}{\overset{-e^-}{\rightleftharpoons}} [(NP_3)Rh(C{\equiv}CR)]^+ \underset{+e^-}{\overset{-e^-}{\rightleftharpoons}} [(NP_3)Rh(C{\equiv}CR)]^{2+}$$

Table III summarizes the redox potentials for the two electron transfers and the differences between the peak potential of each forward response and its directly associated backward response. In accord with the less electron-withdrawing character of the phenyl substituent vs that of the ester group, it is easier to oxidize **1** than **2**.

The ΔE_p parameter, which is a measure of the departure from the electrochemical reversibility as compared to the value of 59 mV expected for a purely reversible one-electron transfer, can qualitatively be interpreted in stereochemical terms (the ferrocene/ferrocenium couple under the same conditions displays a ΔE_p value of 75 mV). In fact, only for purely reversible electron transfers, no significant geometrical reorganization of the molecular frame occurs upon electron addition/removal.[32]

Rh(I)/Rh(II) Redox Change. Generation and ESR Characterization of the Stable Rh(II) Derivatives $[(NP_3)Rh(C{\equiv}CR)]^+$ (R = Ph, CO_2Et). The redox behavior of **1** and **2** is consistent with the chemical reversibility of the Rh(I)/Rh(II) redox changes. It is therefore expected that the Rh(II) species $[(NP_3)Rh(C{\equiv}CR)]^+$ can be easily electrogenerated. As a matter of fact, the exhaustive electrolysis at −0.2 V of **1** in THF (0.2 mol dm^{-3} $[NBu_4]ClO_4$ as supporting electrolyte) affords a one-electron-oxidized greenish solution exhibiting a cyclic voltammetric response qualitatively similar to that shown in Figure 1, but the peak system A/D now appears as due to a reduction process at peak D, accompanied by the reoxidation at peak A in the reverse scan.

(32) Geiger, W. E. *Prog. Inorg. Chem.* **1985**, *33*, 275.

Table IV. X-Band ESR Parameters for the Rh(II) σ-Acetylide Complexes of NP_3 and PP_3 in Dichloromethane

NP_3 Complexes

	300 K		100 K			
	$\langle g \rangle$	$\langle A_P \rangle$[a]	$g_\perp$	$g_\parallel$	$A_\perp$[b]	$A_\parallel$[b]
6	2.062	222 21 14	2.082	2.007	201 21	251
7	2.063	219 17	2.085	2.002	215	

PP_3 Complexes

	300 K				100 K			
	species A[c]		species B[c]					
	$\langle g \rangle$	$\langle A_P \rangle$	$\langle g \rangle$	$\langle A_P \rangle$	$g_\perp$	$g_\parallel$	$A_\perp$	$A_\parallel$
10	2.057	190 21 15	2.057	209 19	2.086	1.996	187 32	243 22
11	2.055	190 21 15	2.053	209 19	2.086	1.995	184 32	243 20
12	2.056	190 21 15	2.054	209 19	2.086	1.999	185 34	240 20

[a] A values in gauss. [b] Due to the poor resolution of the spectra, the coupling constants to the basal phosphorus atoms are average values. [c] Computed values on the basis of the experimental data.

The X-band ESR spectrum of the greenish solution at 300 K consists of a doublet of doublets of doublets centered at $\langle g \rangle$ 2.062 (Figure 2a). The spectrum can be interpreted by using a $S = {}^1/_2$ spin Hamiltonian and can be simulated with three $\langle A_P \rangle$ values of 222, 21, and 14 G, respectively. The spectral pattern is typical of distorted square-pyramidal (SQ) Rh(II) complexes in which the unpaired electron strongly couples to the apical phosphorus ($\langle A_P \rangle$ = 222 G) as it approaches the d_{z^2} SOMO (see Scheme I).[33]

A distortion in the coordination polyhedron is evidenced by the two different $\langle A_P \rangle$ values with the basal phosphorus nuclei. The two largely separated signals exhibit slightly different line widths due to the line-width dependence on the m_i value.[34] The line shape of the spectrum does not show any additional hyperfine structure. In actuality, the coupling constants to rhodium in SQ Rh(II) complexes of this type are generally smaller than those to phosphorus (notice that the narrowest line width is 12 G).[33,35]

The frozen-solution spectrum at 100 K, exhibiting $g_\perp$ (2.082) > $g_\parallel$ (2.007) ≥ 2.000, $A_\parallel$ = 251 G, and $A_\perp$ = 201 G, is fully consistent with the SQ symmetry assigned at room temperature (Figure 2b).[33,35,36] A distorted three-line splitting is present in each perpendicular absorption, which is assigned to interaction with the two nonequivalent basal phosphorus nuclei. The poor resolution of the spectrum does not permit one to precisely determine the $A_{P_{basal}}$ values, for which an average value of 21 G is measured. For the same reason, no value for the parallel absorptions can be provided. The solid-state and frozen-solution ESR spectra are essentially coincident, the only apparent difference being a poorer resolution for the powder spectrum.

Addition of ethanol/*n*-heptane to the electrolyzed solution, followed by slow evaporation of the solvent, precipitates yellow-green microcrystals of $[(NP_3)Rh(C{\equiv}CPh)]ClO_4$ (**6**). The room-temperature and frozen ESR spectra of **6** in THF are coincident with those recorded in the electrolyzed solution, thus indicating that no change has occurred during the crystallization process.

The Rh(I) TBP/Rh(II) SQ conversion nicely supports the electrochemical quasireversibility of the relevant redox change. In this regard, measurements of the formal electrode potential of the Rh(I)/Rh(II) redox change for **1** over the temperature range 10–60 °C in THF solution allow one to compute a reaction entropy ($S°_{Rh(I)} - S°_{Rh(II)}$ = +10.5 eu.[29]

In a fashion identical with that described for the one-electron oxidation of **1**, the exhaustive electrolysis of **2** in THF at the first anodic process permits the isolation of $[(NP_3)Rh(C{\equiv}CCO_2Et)]ClO_4$ (**7**) as a yellow-green powder. The X-band ESR spectra of **7** are very similar to those of **6** but are much less resolved. Detailed ESR data for **7** are reported in Table IV, which collects the experimental X-band ESR parameters for all of the new paramagnetic Rh(II) complexes. The tetrafluoroborate and hexafluorophosphate analogues of **6** and **7**, $[(NP_3)Rh(C{\equiv}CR)]Y$ (R = Ph, Y = BF_4 (**6a**), PF_6 (**6b**); R = CO_2Et, Y = BF_4 (**7a**), PF_6 (**7b**)), can be prepared by chemical oxidation of **1** and **2** with either $AgBF_4$ or $[(C_5H_5)_2Fe]PF_6$. In a typical procedure, the neutral acetylide, dissolved in THF or CH_2Cl_2, is treated with a stoichiometric amount of the appropriate oxidant. The precipitation of the Rh(II) derivative is accomplished by addition of ethanol, followed by slow evaporation of the solvent. All of the Rh(II) σ-acetylides are fairly air-stable in the solid state. They behave as 1:1 electrolytes in deoxygenated 1,2-dichloroethane solutions. The presence of a terminal acetylide ligand in all compounds is shown by typical IR absorptions at ca. 2100 cm^{-1}, which are significantly shifted to higher wavenumbers as compared to those of the Rh(I) analogues (see below) (Table II). Reinforced phenyl vibrations at ca. 1600 cm^{-1} are present in the IR spectra of the phenylacetylides, whereas the carboxyacetylides exhibit absorptions in the proper region for ν(C=O) and ν(C—O—C). All of the compounds are paramagnetic with magnetic moments ranging from 1.90 to 1.85 μ_B, which are diagnostic for one unpaired spin.

Rh(II)/Rh(III) Redox Change. Exhaustive controlled-potential electrolysis of **1** in CH_2Cl_2 solution at the

(33) (a) Bianchini, C.; Laschi, F.; Ottaviani, M. F.; Peruzzini, M.; Zanello, P. *Organometallics* **1988**, *7*, 1660. (b) Bianchini, C.; Laschi, F.; Ottaviani, M. F.; Peruzzini, M.; Zanello, P.; Zanobini, F. *Ibid.* **1989**, *8*, 893.
(34) Wison, R.; Kivelson, D. J. *J. Chem. Phys.* **1966**, *44*, 4445.
(35) Bianchini, C.; Meli, A.; Laschi, F.; Vizza, F.; Zanello, P. *Inorg. Chem.* **1989**, *28*, 227.
(36) Bencini, A.; Gatteschi, D. *Transition Met. Chem. (N.Y.)* **1982**, *8*, 1.

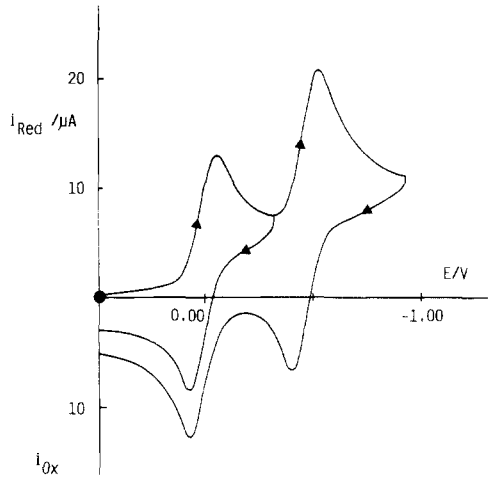

Figure 3. Cyclic voltammogram recorded at a platinum electrode on a deaerated CH_2Cl_2 solution containing **8** (9.50×10^{-4} mol dm^{-3}) and $[NBu_4]ClO_4$ (0.1 mol dm^{-3}) (scan rate 0.2 V s^{-1}).

second anodic process produces a two-electron-oxidized golden yellow solution. The cyclic voltammogram of this solution shows two reduction processes in correspondence to peaks C and D of Figure 1 with peak heights ca. 40% of those of the starting anodic processes. A predominant reduction peak due to an irreversible electron transfer at −1.15 V is also present. Surprisingly, bulk electrolysis in correspondence to this reduction process (working potential −1.2 V) regenerates the starting complex **1**, thereby indicating that the slow reaction that evidently follows the Rh(II)/Rh(III) charge transfer does not involve framework-destroying steps. We ascribe this chemical complication to interaction of the coordinatively and electronically unsaturated complex dications $[(NP_3)Rh(C{\equiv}CPh)]^{2+}$ with the solvent. The Rh(III) complex $[(NP_3)Rh(C{\equiv}CPh)]^{2+}$ is readily formed also by two-electron and one-electron chemical oxidations of **1** and **6b**, respectively, with use of appropriate amounts of $[(C_5H_5)_2Fe]PF_6$ in CH_2Cl_2. As a result, the diamagnetic complex $[(NP_3)Rh(C{\equiv}CPh)](PF_6)_2$ (**8**) is obtained as pale yellow, very hygroscopic microcrystals by adding *n*-hexane. In good agreement with the electrochemical findings, the Rh(II) derivative **6b** and the Rh(I) parent complex **1** are readily prepared by reaction of **8** in THF with 1 and 2 equiv of $LiHBEt_3$, respectively.

Freshly prepared solutions of **8** in CH_2Cl_2 exhibit cyclic voltammograms that are fully complementary with those of the starting Rh(I) acetylides **1** (Figure 3 reports the cyclic voltammogram exhibited by **8** in CH_2Cl_2). The redox pattern of Figure 3 is perfectly complementary with that of Figure 1, thus demonstrating the chemical reversibility of the Rh(I)/Rh(II)/Rh(III) electron-transfer chain. However, cyclic voltammograms of **8** in CH_2Cl_2 solution recorded at different times reveal that a slow reaction occurs, which most likely involves the solvent to form octahedral (OCT) derivatives (see below). After ca. 2 h, the cyclic voltammogram closely resembles that of the two-electron-electrolyzed solution of **1**. Addition of *n*-hexane precipitates **8** in almost quantitative yield. When ethanol is used in the place of *n*-hexane to precipitate the product, pale cream-colored crystals of $[(NP_3)Rh(C{\equiv}CPh)(C_2H_5OH)](PF_6)_2$ (**8a**) are collected. In a similar way, when **1** and **6a** are oxidized by $AgBF_4$ in THF and the reaction products are precipitated with ethanol, the complex $[(NP_3)Rh(C{\equiv}CPh)(C_2H_5OH)](BF_4)_2$ (**8b**) is obtained. Recrystallization of **8** from acetone/ethanol gives the acetone adduct $[(NP_3)Rh(C{\equiv}CPh)(CH_3COCH_3)](PF_6)_2$ (**8c**). The cyclic voltammograms of **8a–c** are identical with each other and similar to that of the species which slowly forms in the two-electron electrochemically oxidized solution of **1**. In addition, bulk electrolysis of **8a–c** in CH_2Cl_2 at −1.2 V regenerates **1**, thus indicating that **8a–c** are chemically connected to **8**.

Identical redox and chemical properties are displayed by the Rh(III) complex cation $[(NP_3)Rh(C{\equiv}CCO_2Et)]^{2+}$, which can be prepared from **2** either by controlled-potential electrolysis in CH_2Cl_2 or by chemical oxidation with appropriate reagents. Depending on the solvent, the following derivatives have been isolated: $[(NP_3)Rh(C{\equiv}CCO_2Et)(C_2H_5OH)](PF_6)_2$ (**9a**), $[(NP_3)Rh(C{\equiv}CCO_2Et)(CH_3COCH_3)](PF_6)_2$ (**9b**), $[(NP_3)Rh(C{\equiv}CCO_2Et)(C_2H_5OH)](BF_4)_2$ (**9c**), and $[(NP_3)Rh(C{\equiv}CCO_2Et)(CH_3COCH_3)](BF_4)_2$ (**9d**).

A useful diagnostic tool to verify the interaction of the Rh(III) dications $[(NP_3)Rh(C{\equiv}CR)]^{2+}$ (R = Ph, CO_2Et) with the solvent is provided by $^{31}P\{^1H\}$ NMR spectroscopy (Table I). In fact, although they invariably exhibit AM_2X spin systems, the $^{31}P\{^1H\}$ NMR spectra of all of the compounds change on going from one solvent to another. In CH_2Cl_2, the spectrum of **8**, which is the only member of the family to be isolated, shows the presence of a unique species. The NMR parameters are consistent with a SQ structure. However, some interaction with CH_2Cl_2 to give an octahedral complex cannot be excluded a priori, especially in view of the redox behavior of the compound. A quite different spectrum is shown by **8** in acetone (Figure 4). At room temperature, the spectrum consists of two broad doublets in a 1:2 ratio. When the temperature is decreased, each doublet begins to split into two components. At 188 K, the higher field signal is well resolved into a pair of doublets of doublets of very different intensities, while the lower field signal splits into a pair of doublets of triplets. The spectra shown in Figure 4 have been nicely computed by considering a nonmutual exchange between two AM_2X configurations having ca. 10:1 populations.[27] Interestingly, all of the compounds of the **8** and **9** families in acetone solution show a ^{31}P NMR behavior of this type, regardless of the solvent used for their preparation or recrystallization, thus indicating that acetone replaces even ethanol in the complex dications. Indeed, the spectra of the ethanol solvates **8a,b** and **9a,c** in CH_2Cl_2 are quite different as compared to those recorded in acetone. No dynamic process on the NMR time scale is now observed over the temperature range 300–193 K, while two species exhibiting AM_2X patterns are present in a ca. 1:1 ratio. As will be discussed in detail also for the PP_3 derivatives (see below), the most straightforward interpretation for the ^{31}P NMR behavior of the present family of Rh(III) σ-acetylides in basic solvents is to consider that two alternative coordination sites may be used to saturate the $[(NP_3)Rh(C{\equiv}CR)]^{2+}$ fragments; i.e. the stable 18-electron configuration at the metal can be attained by setting a fifth ligand trans either to the bridgehead nitrogen or to a terminal phosphorus (Scheme I). In this respect, the fluxional behavior in acetone may be due to an interconversion between the two geometric isomers.

With the exception of a few IR and ^1H NMR bands, especially those related to the counterion and to the substituent on the acetylide ligand, all of the members of the **8** and **9** families exhibit very similar chemical–physical properties. They all are air-stable both in the solid state and in solutions, in which they behave as 1:2 electrolytes. Another important point, which will be discussed in detail in the last section of this paper, regards $\nu(C{\equiv}C)$ of the

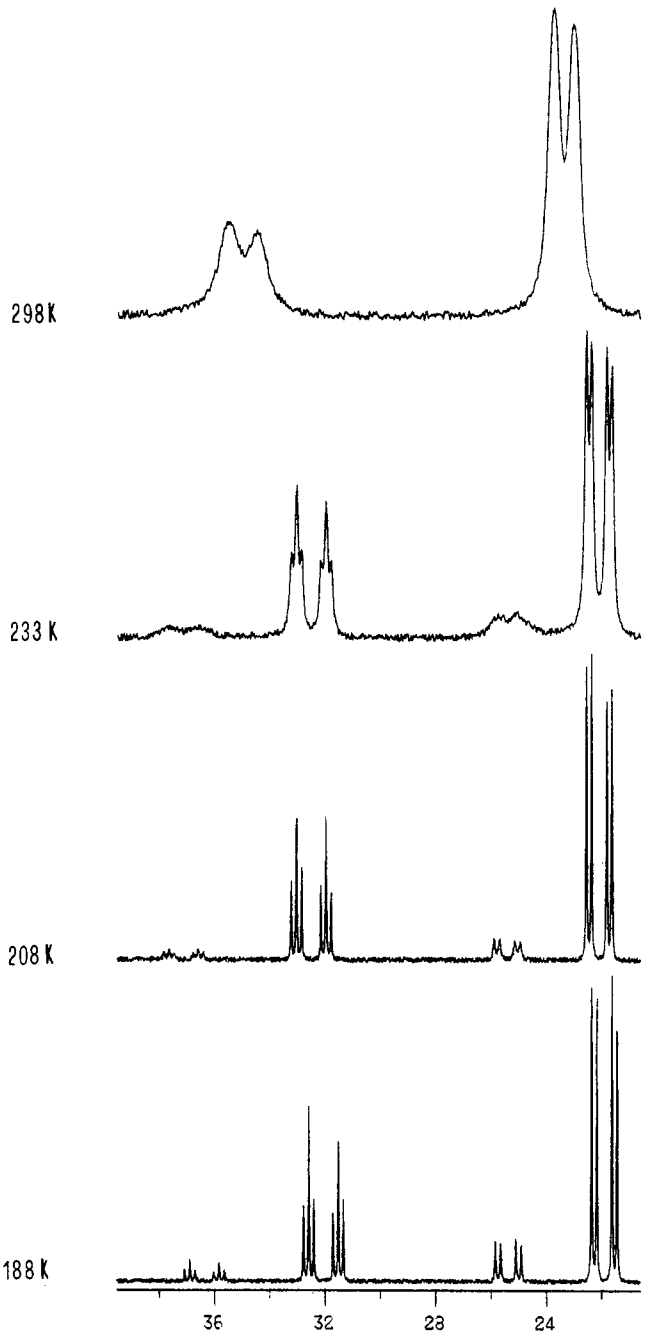

Figure 4. Variable-temperature $^{31}P\{^1H\}$ NMR spectra of **8c** in CD_3COCD_3 (121.42 MHz, 85% H_3PO_4 reference).

acetylide ligands that, in the present family of Rh(III) complexes, is shifted further to higher wavenumbers as compared to those of the Rh(II) derivatives (Table II).

PP_3 Complexes. The PP_3 derivatives **3–5** show a redox behavior qualitatively similar to that reported for **1** and **2**, in that they undergo two sequential one-electron removals. Figure 5 reports the cyclic voltammograms recorded in CH_2Cl_2 solutions of **3** and **4**. The redox potentials for the two oxidation steps in the series **3–5** are summarized in Table III.

Rh(I)/Rh(II) Redox Change. As for the NP_3 σ-acetylides, the first oxidation involves a simple quasireversible one-electron process. Exhaustive electrolysis of **3–5** in CH_2Cl_2 (0.2 mol dm^{-3} $[NBu_4]ClO_4$ as supporting electrolyte) at the first anodic process invariably affords emerald green solutions, which have been studied by ESR techniques. Addition of ethanol/*n*-heptane to the electrolyzed solutions precipitates green microcrystals of $[(PP_3Rh(C{\equiv}CR)]ClO_4$ (R = Ph (**10**), CO_2Et (**11**), CHO (**12**)). As observed for the NP_3 analogues, the room-temperature and frozen-solution X-band ESR spectra of **10–12** are coincident with those recorded for the electrolyzed solutions, thus indicating that no change has occurred during the precipitation. The tetrafluoroborate and hexafluorophosphate derivatives $[(PP_3)Rh(C{\equiv}CR)]Y$ (R = Ph, Y = BF_4 (**10a**), PF_6 (**10b**); R = CO_2Et, Y = BF_4 (**11a**), PF_6 (**11b**); R = CHO, Y = BF_4 (**12a**), PF_6 (**12b**)) can be prepared by chemical oxidation of **3–5** with either $AgBF_4$ in THF or $[(C_5H_5)_2Fe]PF_6$ in CH_2Cl_2. Unlike the NP_3 derivatives **1** and **2**, the PP_3 σ-acetylides are oxidized in benzene solutions by strong protic acids such as $HOSO_2CF_3$. A detailed study of these reactions will be presented in a future article. All of the Rh(II) σ-acetylide complexes belonging to the PP_3 family are paramagnetic with magnetic moments ranging from 1.90 to 1.85 μ_B, as expected for low-spin d^7 rhodium species.[36] They all are fairly stable in the solid state and behave as 1:1 electrolytes in 1,2-dichloroethane solutions. The IR spectra contain ν(C≡C) at ca. 2095 cm^{-1}, which is somewhat higher than ν(C≡C) in the parent Rh(I) acetylides. Typical IR absorptions at 1590, 1670, and 1600 cm^{-1} are readily assigned to the Ph, CO_2Et, and CHO substituents on the acetylide ligands in **10**, **11**, and **12**, respectively.

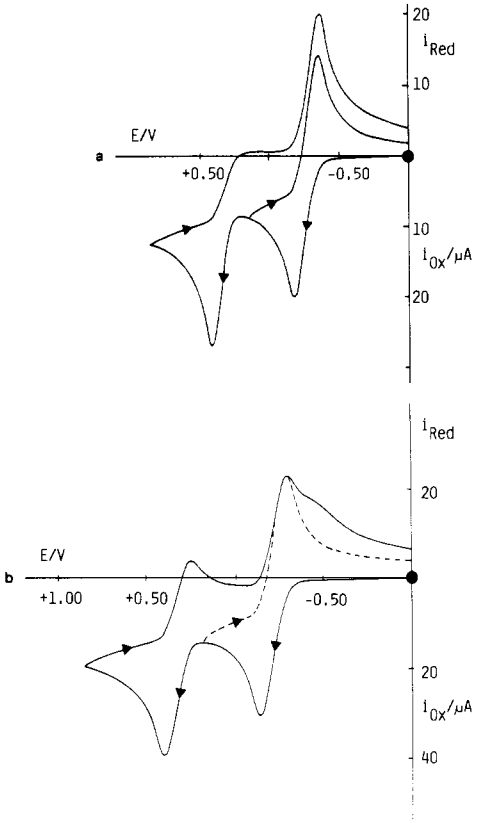

Figure 5. Cyclic voltammograms recorded at a platinum electrode on deaerated CH_2Cl_2 solutions containing $[NBu_4]ClO_4$ (0.1 mol dm^{-3}) and (a) **3** (1.40×10^{-3} mol dm^{-3}) or (b) **4** (2.10×10^{-3} mol dm^{-3}) (scan rate 0.2 V s^{-1}).

At 100 K, the ESR spectra of **10–12** are quite similar to those of the NP_3 complexes **6** and **7** and can be analogously interpreted by using a $S = {}^1/_2$ spin Hamiltonian.[36] The spectroscopic parameters, which are listed in Table IV, are consistent with the presence of a unique species with a distorted SQ symmetry. The spectra are generally better resolved than those of the NP_3 derivatives, and a three-line splitting is now observable also in the parallel absorptions. However, the resolution is still rather poor and the A_P values cannot be precisely determined (Figure 6a shows

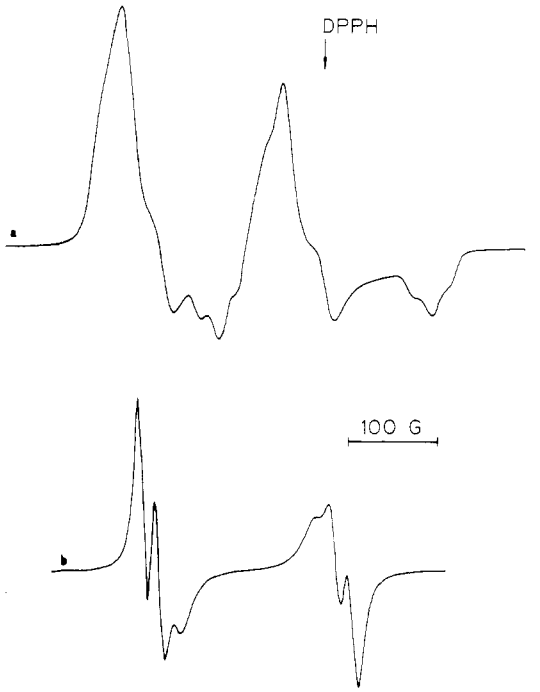

Figure 6. X-Band ESR spectra of $[(PP_3)Rh(C{\equiv}CCO_2Et)]^+$ in CH_2Cl_2 at 300 K (b) and 100 K (a).

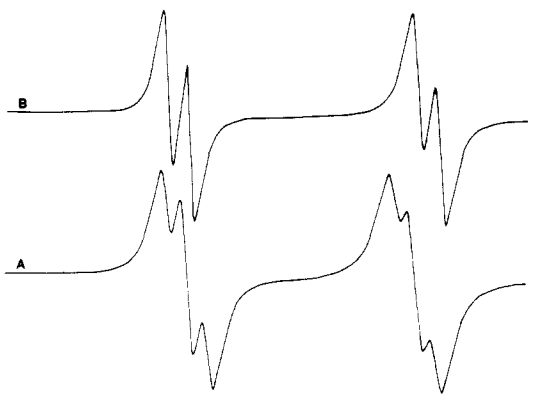

Figure 7. Computed ESR spectra of species A and B of $[(PP_3)Rh(C{\equiv}CCO_2Et)]^+$ in CH_2Cl_2 at 300 K.

the spectrum of **11a** in CH_2Cl_2 at 100 K).

The ESR spectra of **10–12** in fluid CH_2Cl_2 solution are not as readily interpretable as the frozen-solution spectra, since they can be properly computed only by considering the presence in solution of two Rh(II) species, the relative amount of which depends on the temperature. As an example, we report in Figure 6b the experimental spectrum of **11a** at 300 K, which can be simulated as the sum of two subspectra in a ca. 1:1 ratio. The computed line shape of each subspectrum is shown in Figure 7. The ESR spectrum of one of the two species (hereafter species A) consists of a doublet of doublets of doublets. The pattern (ddd) and the spectral parameters ($\langle g \rangle$ = 2.055, $\langle A_{P_{apical}} \rangle$ = 190 G, $\langle A_{P_{basal}} \rangle$ = 15 and 21 G) are quite similar to those found for the NP_3 derivatives **6** and **7** as well as to those previously reported for a number of NP_3 and PP_3 complexes of Rh(II) with distorted SQ structures.[33] The contribution of the second species (hereafter species B) appears as a doublet of doublets centered at $\langle g \rangle$ = 2.053 with $\langle A_{P_{apical}} \rangle$ = 209 G and $\langle A_{P_{basal}} \rangle$ = 19 G. This spectrum is still diagnostic for a SQ complex of Rh(II). However, a remarkable distortion must be present in the coordination polyhedron, as only one coupling constant to phosphorus is observed.[37]

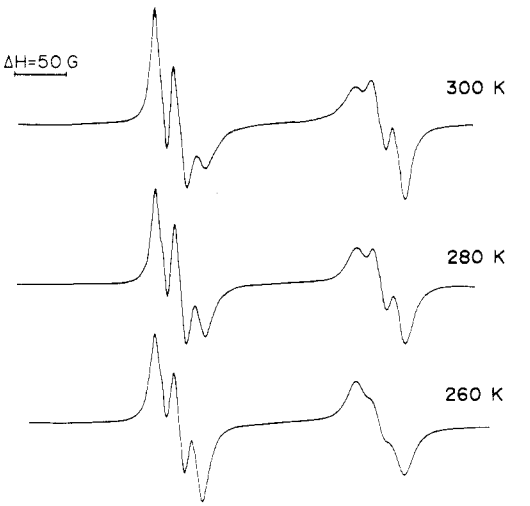

Figure 8. X-Band ESR spectra of **11a** in CH_2Cl_2 at 300, 280, and 260 K.

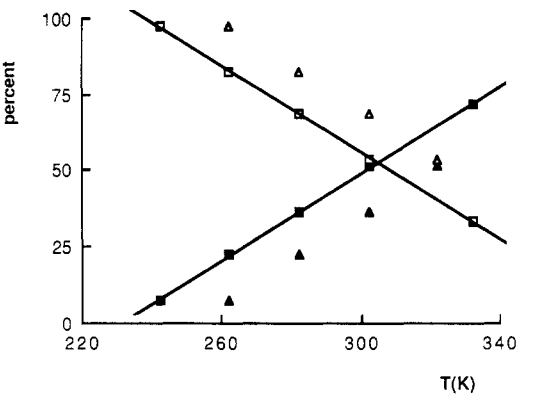

Figure 9. Plot of the percentage of isomers A and B of $[(PP_3)Rh(C{\equiv}CR)]^+$ against the temperature ((□) ddd pattern, for A, (■) dd pattern for B, R = CO_2Et, CHO; (△) ddd pattern, for A, (▲) dd pattern for B, R = Ph).

When the temperature is lowered, the contribution due to species A increases while that of species B decreases with no change in the ESR parameters, as is clearly shown in Figure 8, which reports the spectra of **11a** at 300, 280, and 260 K. In contrast, increasing the temperature increases the amount of species B in solution. The process is fully reversible.

Plotting the relative percentage of each species (as determined by computing the ESR spectra) against the temperature shows that, above 365 K and below 240 K, only one species is present (Figure 9). This result nicely fits with the finding of a unique species in the frozen solution. Unfortunately, it was not possible to record ESR spectra above 300 K because of the extensive decomposition of the compound. Identical behavior is exhibited by the formylacetylide and phenylacetylide derivatives **10** and **12**, with the only difference being that, for the latter complex, equimolar amounts of species A and B are present in solution at a slightly higher temperature, ca. 320 K.

On the basis of all of these data and with recollection of the behavior of the NP_3 acetylides of Rh(III), it is reasonable to conclude that the $[(PP_3)Rh(C{\equiv}CR)]^+$ cations can exist in solution as two isomeric forms in a ratio that depends on the temperature. The existence of geo-

(37) Bianchini, C.; Laschi, F.; Meli, A.; Peruzzini, M.; Zanello, P.; Frediani, P. *Organometallics* **1988**, *7*, 2575.

metric isomers for SQ complexes of the $(PP_3)Rh$ system is not new. In particular, it has been previously reported that the triflate complex $[(PP_3)Rh(SO_3CF_3)]$ exists in ambient-temperature solution as a 1:1 mixture of two species that differ from each other only in the relative position of the triflate ion, i.e. trans either to the bridgehead phosphorus or to a terminal phosphorus.[38] A similar interpretation was given to explain the presence of two species of the Rh(II) complex $[(PP_3)Rh(CN)]^+$ in room-temperature solutions.[33b] Accordingly, the solution behavior of **10–12** can be interpreted in terms of a temperature-dependent equilibrium between two species having SQ symmetry. These may interconvert into each other by simply shifting the position of the σ-acetylide ligand, i.e. trans either to the bridgehead phosphorus or to the basal phosphorus (Scheme I).

The structural formulations of Scheme I are obviously idealized, as the ESR spectra are clearly consistent with a remarkable distortion in the coordination polyhedra. In the absence of more detailed studies, it is not possible to determine which structure belongs to which ESR spectrum. However, it is worth noticing that the coordination polyhedra of the very few five-coordinate PP_3 complexes of d^7 metals which have been authenticated by X-ray methods[39] are invariably described as distorted square pyramids with the bridgehead phosphorus and the fifth coligand lying trans to each other in the basal plane. In this respect, the frozen and low-temperature (<240 K) species is most likely the one with the acetylide ligand located trans to the bridgehead phosphorus atom.

Rh(II)/Rh(III) Redox Change. Unlike the case for the NP_3 complexes, the chemical complication following the 1+/2+ redox change now appears to be very fast and depends on the R substituent. In fact, the analysis of the cyclic voltammetric responses with scan rates shows that for R = Ph, no associated rereduction peak is detected even at the scan rate of 10 V s^{-1}, thus indicating a very fast coupled reaction ($t_{1/2}$ < 0.05 s). In contrast, for R = CHO and CO_2Et, the i_{pc}/i_{pa} ratio reaches the value of 1 at the scan rates of 10 and 2 V s^{-1}, respectively. This means that in both cases the chemical complications proceed within the time window of the cyclic voltammetric technique. Provided that there is a first-order coupled homogeneous reaction,[40] a rough evaluation of the half-life of the dicationic species is the following: R = CHO, $t_{1/2} \cong 1$ s; R = CO_2Et, $t_{1/2}$ = 4 s. The occurrence of a fast chemical reaction involving the dications $[(PP_3)Rh(C{\equiv}CR)]^{2+}$ (R = Ph, CO_2Et, CHO) is demonstrated also by the two-electron chemical oxidation of the starting σ-acetylides **3–5**. As an example, Figure 10 shows the cyclic voltammetric response obtained from a CH_2Cl_2 solution of **13**.

An irreversible reduction process at E_p = −0.8 V is evident, which generates in the reverse scan a voltammetric profile quite identical with that exhibited by **3**. This behavior substantially parallels that found after exhaustive two-electron anodic oxidation of the corresponding NP_3 derivative **1**, but now the chemical complication following the two-electron oxidation is not a secondary process. Therefore, we decided to study the chemical and electrochemical properties of some of the Rh(III) members of the PP_3 family prepared by the usual chemical methods, i.e oxidation of the $[(PP_3)Rh(C{\equiv}CR)]$ acetylides **3** and **4**, with

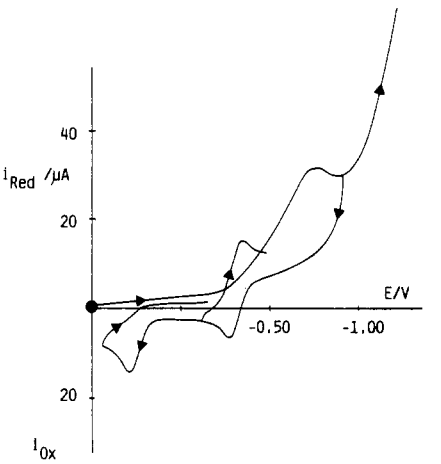

Figure 10. Cyclic voltammogram recorded at a platinum electrode on a deaerated CH_2Cl_2 solution containing $[NBu_4]ClO_4$ (0.1 mol dm^{-3}) and a sample (20 mg/20 mL) of chemically oxidized **3** (see text) (scan rate 0.2 V s^{-1}).

$[(C_5H_5)_2Fe]PF_6$ in CH_2Cl_2 or with $AgBF_4$ in THF. In no case was it possible to isolate the dication $[(PP_3)Rh(C{\equiv}CR)]^{2+}$ without solvent molecules; in contrast, by addition of ethanol the pale yellow or off-white derivatives $[(PP_3)Rh(C{\equiv}CR)(C_2H_5OH)]Y_2$ were prepared in good yields (R = Ph, Y = PF_6 (**13**), BF_4 (**13a**); R = CO_2Et, Y = PF_6 (**14**), BF_4 (**14a**)).

The cyclic voltammograms of all of the members of the **13** and **14** families are characterized by an irreversible cathodic reduction in the range −0.8 to −1.2 V, which regenerates the corresponding Rh(I) σ-acetylides upon bulk electrolysis.

As for the analogous Rh(III) derivatives of NP_3, the $^{31}P\{^1H\}$ NMR spectra of the σ-acetylides **13** and **14** are strongly dependent on the solvent (Table I). Once again, acetone displaces ethanol from the metal, whereas the bonding interaction between ethanol and the $[(PP_3)Rh(C{\equiv}CR)]^{2+}$ dications seems to be maintained in CH_2Cl_2 solution. As a matter of fact, while the recrystallization of **13** and **14** from acetone/ethanol mixtures yields the acetone adducts $[(PP_3)Rh(C{\equiv}CR)(CH_3COCH_3)](PF_6)_2$ (R = Ph (**15**), CO_2Et (**16**)), the compounds remain unchanged when they are recrystallized from CH_2Cl_2/ethanol mixtures.

The spectra of the phenylacetylide complex **13a** in acetone and dichloromethane are reported in Figures 11 and 12, respectively. In acetone, two species in a ca. 1:1 ratio are present, each of which exhibits an AM_2QX spin system (Figure 11a shows the experimental spectrum in the region 44–37 ppm). The spectrum can be computed as the 1:1 sum of two contributions (Figure 11c,d), each of which constitutes the M_2Q portion of an AM_2QX pattern. The A portions of both spectra resonate at very low field, as expected for the bridgehead phosphorus atoms of PP_3.

A quite different $^{31}P\{^1H\}$ NMR spectrum is found in CH_2Cl_2 solution. First, only one species is present. Second, the spectrum is temperature-dependent. At room temperature, the spectrum consists of two very greatly separated doublets with 1:3 intensities. Such a pattern is typical of fluxional rhodium complexes, in which the three terminal phosphorus donors of PP_3 exchange very rapidly.[38,41] When the temperature is decreased, the higher field doublet is resolved into a complicated second-order pattern, which only at 213 K appears as the quasi-first-order

(38) Bianchini, C.; Masi, D.; Meli, A.; Peruzzini, M.; Zanobini, F. *J. Am. Chem. Soc.* **1988**, *110*, 6411.
(39) (a) Di Vaira, M. *J. Chem. Soc., Dalton Trans.* **1975**, 2360. (b) Orlandini, A.; Sacconi, L. *Inorg. Chem.* **1976**, *15*, 78.
(40) Brown, E. R.; Sandifer, J. R. In *Physical Methods of Chemistry Electrochemical Methods*; Rossiter, B. W., Hamilton, J. F., Eds.; Wiley: New York, 1986; Vol. II, Chapter IV.
(41) Bianchini, C.; Meli, A.; Peruzzini, M.; Ramirez, J. A.; Vacca, A.; Vizza, F.; Zanobini, F. *Organometallics* **1989**, *8*, 337.

Table V. Redox Potentials for Rh(I)/Rh(II) Recox Changes Exhibited by [(L)RhX] Complexes (L = NP_3, PP_3; X = Cl, H, C≡CR, CN, CO)

	X						
	Cl	H	C≡CPh	C≡COOEt	C≡CCHO	CN	CO[a]
$[(NP_3)RhX]$	−0.47[b]	−0.44[c]	−0.45[b]	−0.26[b]		−0.19[b]	>+0.5[b,c]
			−0.43[c]	−0.26[c]		−0.19[c]	
$[(PP_3)RhX]$	−0.31[b]	0.31[c]	−0.29[b]	−0.21[b]	−0.17[b]	−0.13[b]	>+0.5[b,c]
			−0.27[c]	−0.19[c]	−0.16[c]	−0.12[c]	

[a] The carbonyl complex is monocationic. [b] CH_2Cl_2 solution. [c] THF solution.

M_2Q portion of an AM_2QX spin system (Figure 12).

A quite similar NMR behavior is displayed by the ethoxycarbonyl derivatives **14** and **16**.

As we have previously suggested for the Rh(III) σ-acetylides of NP_3, the unusual dependence of the ^{31}P NMR spectra of the $[(L)Rh(C{\equiv}CR)]^{2+}$ systems on the solvent is a consequence of the unsaturated nature of these dications. In general, however, even for those solvents such as acetone, which forms fairly stable adducts, the complexes are not as rigid as commonly found for octahedral Rh(III) complexes of formula [(L)Rh(X)(Y)] (L = NP_3, PP_3; X, Y = monofunctional ligand),[25,38,41,42] thereby indicating that both the fluxionality and the existence of coordination isomers may be due to a weak bonding interaction such as that with solvent molecules.

All of the Rh(III) σ-acetylide complexes belonging to the **13** and **14** families are stable in the solid state and in solution, in which they behave as 1:2 electrolytes. The presence of a terminal acetylide ligand in all compounds is evidenced by medium-intensity IR bands that are significantly shifted to higher wavenumbers as compared to those of the Rh(II) analogues.

π-Acceptor Ability of the σ-Acetylide Ligands. Any absolute measurement of the π-acceptor abilities of the σ-acetylide ligands in the compounds herein presented is beyond the purposes of this paper. However, the presence of a metal → acetylide π* interaction in the HOMO can be probed and also empirically evaluated by comparing the stretching frequencies ν(C≡C) and the redox potentials $E°'$ within the present family of σ-acetylide complexes of rhodium as well as a larger family of TBP Rh(I) complexes with the NP_3 and PP_3 ligands. The relationship between ν(C≡C) and back-donation is determined by the fact that an effective transfer of electrons from the metal to the acetylide ligand is expected to increase the M–C bond order, decrease the C–C bond order, and ultimately, drive the C–C stretching frequencies down.[1a,24,43] However, as the extent of back-donation depends on a number of different factors such as the nature of the acetylide substituents and of the other coligands, the formal oxidation state of the metal, and the symmetry of the complex molecule, the use of ν(C≡C) as a diagnostic tool for evaluating the metal → acetylide π* interaction proves significant only when a comparison is made within compounds that are as much as possible related to each other. This prerequisite is certainly fulfilled by the members of a redox family as the σ-acetylide complexes of NP_3 and PP_3 or the redox pairs $[Mo(C{\equiv}CR)(dppe)(\eta\text{-}C_7H_7)]/[Mo(C{\equiv}CR)(dppe)(\eta\text{-}C_7H_7)]^+$ (R = Ph, Bu^t; dppe = $Ph_2PCH_2CH_2PPh_2$), for which the absence of dπ (metal) → π* (ligand) transfer was diagnosed on the basis of a small decrease in ν(C≡C).[43] The IR data reported in Table II clearly show that, as one goes from the Rh(I) σ-acetylides **1–5** to their Rh(III) derivatives of the **8**, **9** and **13**, **14** families, ν(C≡C) constantly increases by ca. 30 and 10 cm^{-1}

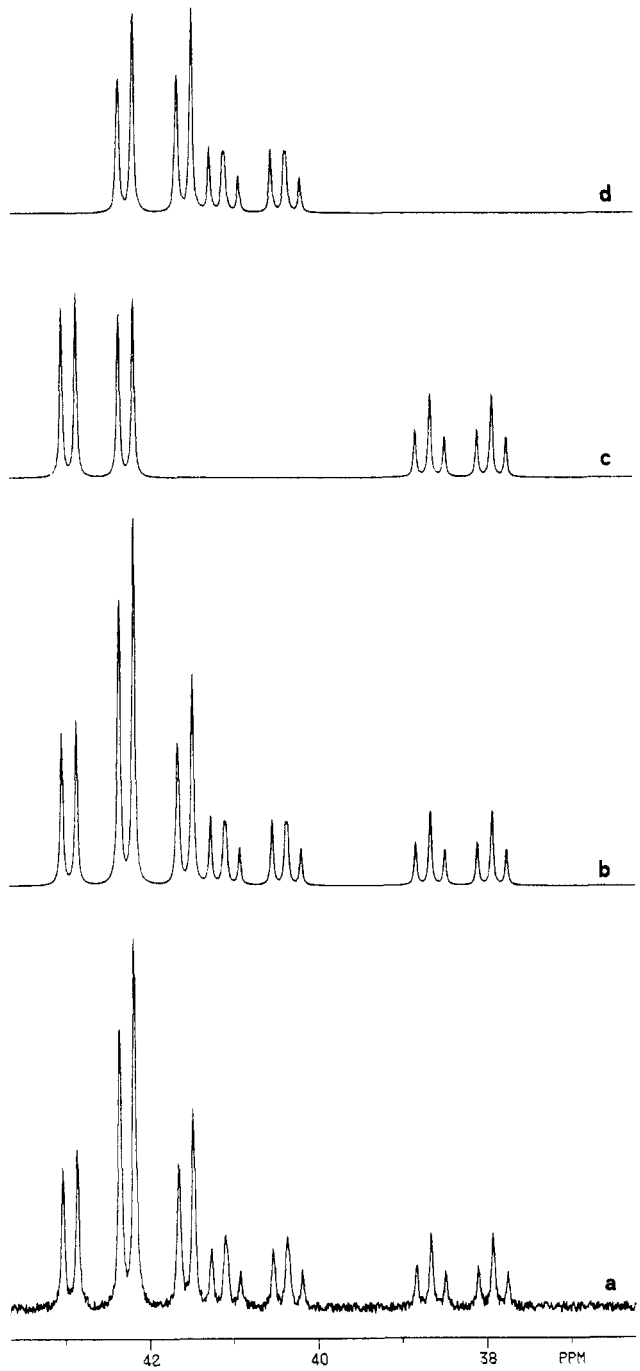

Figure 11. (a) $^{31}P\{^1H\}$ NMR experimental spectrum in acetone of **13a** in the region 44–37 ppm (298 K, 121.42 MHz, 85% H_3PO_4 reference). (b) Computed spectrum as the 1:1 sum of the two contributions shown in (c) and (d).

(42) (a) Bianchini, C.; Meli, A.; Peruzzini, M.; Zanobini, F. *J. Chem. Soc., Chem. Commun.* **1987**, 971. (b) Bianchini, C.; Mealli, C.; Peruzzini, M.; Zanobini, F. *J. Am. Chem. Soc.* **1987**, *109*, 5548. (c) Bianchini, C.; Mealli, C.; Peruzzini, M.; Vizza, F.; Zanobini, F. *J. Organomet. Chem.* **1988**, *346*, C53. (d) Bianchini, C.; Peruzzini, M.; Vizza, F.; Zanobini, F. *Ibid.* **1988**, *348*, C9. (e) Di Vaira, M.; Stoppioni, P.; Peruzzini, M. *Ibid.* **1987**, *333*, C53.

(43) Adams, J. S.; Bitcon, C.; Brown, J. R.; Collison, D.; Cunningham, M.; Whiteley, M. W. *J. Chem. Soc., Dalton Trans.* **1987**, 3049.

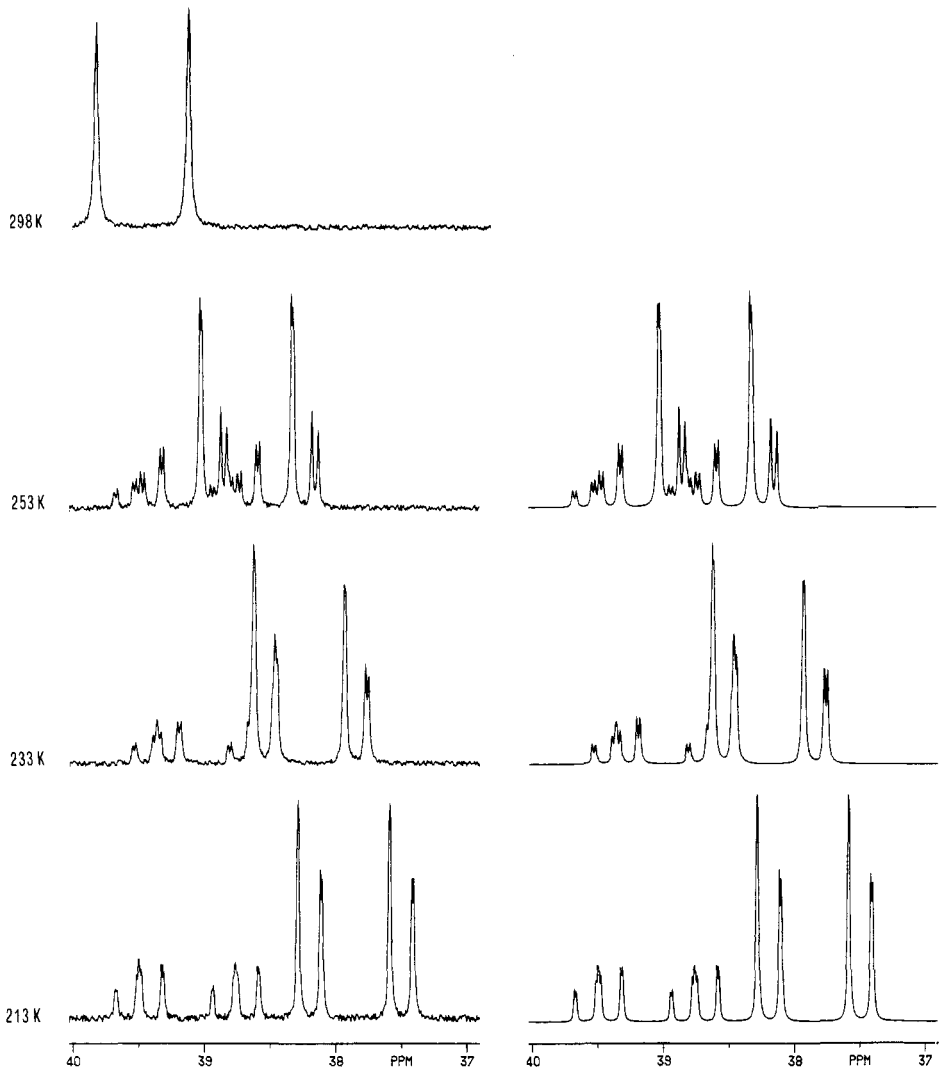

Figure 12. Variable-temperature $^{31}P\{^1H\}$ NMR spectra of **13a** in CH_2Cl_2 in the region 40–37 ppm (121.42 MHz, 85% H_3PO_4 reference).

upon one- and two-electron oxidation, respectively. It is therefore reasonable to conclude that back-donation makes an important contribution to the description of the metal–acetylide bonding in the Rh(I) complexes **1–5** and in the Rh(II) derivatives as well. These experimental results nicely fit in the theoretical framework, since TBP d^8 metal fragments carry two occupied $d\pi$ orbitals with the appropriate symmetry to interact with the two empty π^* orbitals of the acetylide ligand. Both electronic (d^8 vs d^7 metal) and symmetry (TBP vs SQ structure) arguments can contribute to explain the much higher $\Delta\nu(C{\equiv}C)$ value observed for the Rh(I)/Rh(II) redox change (30 vs 10 cm^{-1}). In fact, in the TBP geometry, the metal carries two $d\pi$ orbitals with the proper symmetry to interact with the two acetylide π^* orbitals, whereas in the SQ geometry, only one metal orbital can do that.

Another useful and relatively simple diagnostic tool to evaluate the extent of back-donation in σ-acetylide metal complexes is provided by the redox potentials $E^{\circ\prime}$ relative to the one-electron oxidation.[24,43,44] In fact, at least in principle, any electron transfer from metal to ligand is expected to make the complexes more difficult to oxidize. We decided, therefore, to measure the redox potential for the Rh(I)/Rh(II) redox change of TBP Rh(I) complexes with NP_3 and PP_3 in which the π-acceptor ability of the fifth axial ligand was varied as systematically as possible. The following complexes were investigated: [(L)RhCl],[38] [(L)RhH],[38] [(L)Rh(CN)],[33b] and [(L)Rh(CO)]BPh_4[38] (L = NP_3, PP_3). The data are collected in Table V. These clearly show that, as one goes from ligands with no π-acceptor ability, such as Cl^- or H^-, to carbonyl, which is known to easily accept electron density via π interaction, the $E^{\circ\prime}$ potentials for the Rh(I)/Rh(II) redox change increase in the order Cl > H > C≡CR > CN > CO. Significantly, the σ-acetylide compounds are located midway between the hydride and cyanide congeners, with $E^{\circ\prime}$ values that depend on the electron-withdrawing character of the acetylide substituent. Of particular interest are the relative positions of the acetylide and cyanide ligands, which are placed in the spectrochemical series near each other and enter into π and σ bonding as well with transition metals.[45] Assuming the reliability of the $E^{\circ\prime}$ method, the cyanide ligand is assigned a greater π-acceptor ability as compared to that of terminal acetylides.

Acknowledgment. Thanks are due to F. Zanobini and to P. Innocenti for technical assistance.

(44) Bitcon, C.; Whiteley, M. W. *J. Organomet. Chem.* **1987**, *336*, 385.

(45) Sharpe, G. A. In *Comprehensive Coordination Chemistry*; Wilkinson, G., Gillard, R. D., McCleverty, J. A., Eds.; Pergamon Press: Oxford, England, 1987; Vol. II, Chapter 12.1.